Highly Dispersed Phosphate Supported in a Binary Silica−Titania Matrix: Preparation and Characterization

Antonio A. S. Alfaya and Yoshitaka Gushikem*

Instituto de Quimica, Unicamp, CP 6154, 13083-970 Campinas, SP, Brazil

Sandra C. de Castro

Instituto de Física Gleb Wataghin, CP 6165, 13083-970 Campinas, SP, Brazil

Received October 15, 1997. Revised Manuscript Received December 30, 1997

Titanium phosphate supported in a mixed oxide matrix was prepared by reacting SiO_2/TiO_2, obtained from the sol−gel process, with phosphoric acid. HPO_4^{2-} is the species present in the matrix, and it is immobilized by the Ti−O−P bond on the surface. The titanium phosphate is highly and homogeneously dispersed in the SiO_2/TiO_2 matrix, with the domain of titanium oxide particles about 1 nm, estimated from the UV absorption band threshold. The specific surface areas, determined by the BET multipoint method, changed between 397 and 755 $m^2\ g^{-1}$ and the average pore volumes between 0.38 and 0.63 mL g^{-1} for samples prepared with different contents of titanium phosphate. The titanium hydrogenphosphate is thermally very stable and showed a high proton exchange capacity between 0.50 and 1.10 mmol g^{-1}.

Introduction

Titanium(IV) phosphate is known for its excellent ion-exchange and electrical conductivity properties.[1,2] The preparation procedure of this material normally involves the mixture of titanium(IV) oxide and phosphoric acid in solution, with separation of the resulting precipitated solid by filtration. However, depending on the working conditions, many different products can be formed because of the highly hydrolyzable tetravalent cation with different degrees of polymerization during the precipitation with hydrogen phosphate ion.[3] The method may not be convenient because, from a practical point of view, in most cases it leads to the formation of a fine powder with a poor mechanical resistance, low specific surface area, and low thermal stability.[4]

The sol−gel process is a convenient method to prepare binary oxides of the type SiO_2/M_xO_y, with a high degree of homogeneity and purity.[5−9] SiO_2/TiO_2 has been prepared by this process, aiming for its use in catalytic reactions.[10−14] This method also allows one to obtain material with a high concentration of the Ti(IV) in the matrix, which may be of great interest.[1] This work reports the preparation of titanium(IV) phosphate starting from SiO_2/TiO_2, obtained by the sol−gel process, and further reaction with phosphoric acid in order to obtain a material in which the titanium phosphate is highly dispersed, presenting a high proton exchange capacity associated with good mechanical resistance. The degree of the particle dispersion in the matrix, the thermal stability, the proton-exchange capacity, and the nature of the species present in the material were investigated. Interest in preparing material with such characteristics is related to its potential use as a chemical sensor.[15−17]

Tests carried out with an electrode made with {SiO_2/TiO_2/phosphate/redox dye} have shown that the redox dyes, methylene blue (MB) and Meldola's blue (MeB), can mediate electron-transfer processes.[18] Between pH 2 and 7 the adsorbed dyes presented the midpoint potentials, E_m (against SCE, saturated calomel electrode), at −100 mV for MB and 50 mV for MeB. In contrast, for dyes adsorbed on carbon, in the pH range between 2 and 7, the carbon paste/dye electrode E_m (against SCE) changed between the following values: (a) MB −250 and −25 mV[16] and (b) MeB −180 to 0 mV.[19] The almost constant values for E_m for both

(1) Clearfield, A. *Inorganic Ion Exchange Materials*; CRC Press Inc.: Boca Raton, FL, 1982.
(2) Roca, S.; Airoldi, C. *Thermochim. Acta* **1996**, *284*, 289.
(3) Dolmatov, Y. D.; Bulavina, Z. N.; Dolmatov, M. Y. *Radiochim. Acta* **1972**, *14*, 562.
(4) Soria, J.; Iglesias, J. E.; Sanz, J. *J. Chem. Soc., Faraday Trans.* **1993**, *89*, 2515.
(5) Brinker, C. J.; Scherer, G. W. *The Physics and Chemistry of Sol−Gel Processing*; Academic Press Inc.: San Diego, 1990.
(6) De Lange, R. S. A.; Hekkenk, J. H. A.; Kleizer, K.; Burggraaf, A. J. *J. Non-Cryst. Solids* **1995**, *191*, 1.
(7) Schraml-Marth, M.; Walther, K. L.; Wokaun, A.;. Handy, B. E.; Baiker, A. *J. Non-Cryst. Solids* **1992**, *143*, 93.
(8) Haereid, S.; Dahle, M.; Lima, S.; Einarsrud, M. A. *J. Non-Cryst. Solids* **1995**, *186*, 96.
(9) Salvado, M. J. M.; Margaça, F. M. A.; Teixeira, J. *J. Non-Cryst. Solids* **1993**, *163*, 115.
(10) Itoh, M.; Hattore, H.; Tanabe, K. *J. Catal.* **1974**, *35*, 225.
(11) Ko, E. I.; Chen, J. P.; Weissman, J. G. *J. Catal.* **1987**, *105*, 511.
(12) Nakabayashi, H. *Bull. Chem. Soc. Jpn.* **1991**, *65*, 914.
(13) Sohn, J. R.; Jang, H. J. *J. Catal.* **1991**, *132*, 563.
(14) Imamura, S.; Tarumoto, H.; Ishida, S. *Ind. Eng. Chem. Res.* **1989**, *28*, 1449.
(15) Kubota, L. T.; Gouvea, F.; Andrade, A. N.; Milagres, B. G.; Neto, G. O. *Electrochim. Acta* **1996**, *41*, 1465.
(16) Pessôa, C. A.; Gushikem, Y.; Kubota, L. T.; Gorton, L. *J. Electroanal. Chem*. 1**997**, *431*, 23.
(17) Pessôa, C. A.; Gushikem, Y.; Kubota, L. T. *Electroanalysis* **1997**, *9*, 800.
(18) Urbano, C. F.; Gushikem, Y., unpublished results.

S0897-4756(97)00679-0 CCC: $15.00 © 1998 American Chemical Society
Published on Web 02/19/1998

Table 1. Chemical Analyses of Mixed Oxides and Phosphate Incorporated Mixed Oxides, Specific Surface Area, and Average Pore Volume

samples	Ti/wt %	P/wt %	S_{BET}/m^2 g^{-1}	V_p/mL g^{-1}
ST1	7.7		755	0.63
STP1	7.3	1.5	631	0.61
ST2	11.6		607	0.52
STP2	10.8	2.2	465	0.41
ST3	15.4		587	0.47
STP3	14.0	3.1	397	0.38

materials, {SiO_2/TiO_2/phosphate/redox dye}, is very important from the practical point view since they can be used to prepare chemical sensors for real samples, where the pH plays an important role and cannot be change in order to optimize the electrode response.

Experimental Section

Gel Preparation. The silica/titania mixed oxides, SiO_2/TiO_2, with different compositions, were prepared by the sol−gel technique according to the following procedures: 11.4 mL of 0.8 mol L^{-1} HNO_3 were added to 250 mL of a 1:1 (v/v) tetraethyl orthosilicate (Aldrich)−ethanol solution (solution A). This solution was refluxed for 2.5 h, after which 500 mL of a 0.12 mol L^{-1} tetrabutyl orthotitanate (Aldrich)−ethanol solution were added. The mixture was stirred for 2 h at room temperature, and 64 mL of 0.6 mol L^{-1} HNO_3 was slowly added. The resulting gel was dried at 383 K for 48 h, ground in a mortar, sieved to a particle size of 0.25 mm, and finally calcined at 773 K for 120 h, under an air flow. Two samples having different quantities of TiO_2 were also prepared by adding to solution A, 500 mL of 0.20 or 0.29 mol L^{-1} tetrabutyl orthotitanate−ethanol solutions. The sequence of these preparations were the same as previously described.

Preparation of Phosphate Supported in the SiO_2/TiO_2 Matrix. Phosphate was prepared by immersing 4 g of SiO_2/TiO_2 in 50 mL of ∼0.3 mol L^{-1} phosphate solution. The mixture was shaken for 8 h. The solid was filtered, washed, and dried at 353 K.

Chemical Analyses. The sample was analyzed by adding, slowly, a 40 wt % solution of HF until complete dissolution of the solid. The resulting solution was diluted with 100 mL of water, and concentrated NH_4OH was added until precipitation of the hydrous titanium oxide. The solid was allowed to stand for 3 h, filtered and washed with water. The solid was calcined at 1073 K and weighed as TiO_2. The solution phase was acidified with sulfuric acid, and the volume adjusted. The quantity of phosphorus was determined spectrophotometrically using the molybdenum blue method. The results of the analyses are presented in Table 1.

Specific Surface Area and Average Pore Volume. The specific surface area, S_{BET}, was determined by the BET multipoint technique on a Micromeritcs Flow Sorb II 2300 connected to a flow controller. The average pore volume, V_p, of the samples was determined by the mercury intrusion technique on a Micromeritcs Pore Size 9320 system.

Infrared Spectra. The infrared spectra of the KBr/material pressed disk (5 wt %) were obtained on a Bomen MB series FT-IR spectrophotometer. Spectra with 200 cummulative scans were recorded.

UV−Visible Spectra. The electronic transition spectra of the solid samples were obtained by suspending the solid in spectra-grade CCl_4, using a cell with 0.1 cm path length. Good-quality spectra were obtained since the diffraction index of the solid and liquid phases were very close, minimizing radiation scattering. A Beckman DU-640 equipment was used.

Scanning Electron Microscopy (SEM). The SEM images were obtained by dispersing the sample on a double face conducting tape fixed on a brass support. The sample was coated with graphite using the deposition technique using a sputter low voltage LVC 76 from Plasma Science Inc. The microscope used was a JEOL JSM T-300 connected to a secondary electron detector and to an X-ray dispersive energy analyzer from Northern.

X-ray Photoelectron Spectroscopy (XPS). XPS of the samples were obtained using an aluminum anode (Al Kα = 1486.6 eV radiation) at a pressure of 2×10^{-7} Torr on a McPherson ESCA-36 spectrometer. The number of binding energy peaks was determined by the deconvolution process. The atomic ratios were estimated by integrating the areas under the peaks using the corresponding Scofield cross sections for each atomic level of each atom.[20] The binding energies of the atoms were calibrated against a C 1s of 284.6 eV.[21]

CP-MAS ^{31}P NMR. The cross-polarizing magic angle spinning NMR spectra of the solids were obtained at room temperature on a Bruker AC300P spectrometer operating at 121 MHz. A sequencial pulse with contact time of 1 ms, 2 s intervals between the pulses, and acquisition times of 11 ms were the conditions used. Phosphoric acid (85 wt %) was used as reference.

X-ray Diffraction. The X-ray diffraction patterns were obtained using a Shimadzu XD-3A diffractometer. The following conditions were used: radiation of Cu Kα (λ = 0.154 nm) at 30 kV, current of 20 mA and scan rate of 2° min^{-1}.

Thermogravimetric Analysis (TGA) and Differential Scanning Calorimetry (DSC). The TGA curves were obtained between 273 and 1223 K with a heating rate of 5 K min^{-1} under an argon flow. The DSC curves were obtained between 273 and 873 K, with heating rate of 5 K min^{-1}. A Du Pont 9900 equipment was used.

Results and Discussion

Characteristics of the Material. Table 1 shows the results of the chemical analyses for mixed oxides and phosphate-incorporated mixed oxides, as well as the specific surface areas and average pore volumes. The notation ST refers to SiO_2/TiO_2 mixed oxides and STP to the phosphate-incorporated mixed oxides. The specific surface areas (in m^2 g^{-1}) of ST decreased as the content of TiO_2 in the matrixes increased as follow: ST1 = 755, ST2 = 607, and ST3 = 587. By incorporating the phosphate ion in SiO_2/TiO_2, the specific surface area also decreased, i.e., 631, 465, and 397 m^2 g^{-1} for STP1, STP2, and STP3, respectively, and consequently, the average pore volumes also decreased.

The proton exchange capacities determined by acid−base titration were (in mmol g^{-1}): STP1 = 0.50, STP2 = 0.70, and STP3 = 1.10.

Information on the interaction of TiO_2 with the SiO_2 matrix are given by the IR spectra. The SiO stretching frequency, ν(SiO), of the silica surface SiOH group observed at 970 cm^{-1} [22] is slightly shifted to lower frequency, 951 cm^{-1}, in ST samples. The origin of this shift is well-known and is assigned to the ν(SiO) of Si−O−Ti bond.[6,23,24] The other bands observed at 803 cm^{-1} for SiO_2 and at 800 cm^{-1} for SiO_2/TiO_2, are barely affected because they are due to the ν(SiO) of Si−O−Si bond. In phosphate incorporated samples, it is not

(19) Gorton, L.; Torstensson, A.; Jaegfeldt, H.; Johansson, G. *J. Electroanal. Chem.* **1984**, *161*, 103.

(20) Scofield, J. H. *J. Electron. Spectrosc. Relat. Phenom.* **1976**, *8*, 129.

(21) Dilks, A. Characterization of Polymers by ESCA. In *Developments in Polymer Characterization*; Applied Science Publishers: London, 1980.

(22) Kawano, Y.; Denofre, S.; Gushikem, Y. *Vibrat. Spectrosc.* **1994**, *7*, 293.

(23) Negrishi, N.; Fujii, T.; Anpo, M. *Langmuir* **1993**, *9*, 3320.

(24) Hutter, R.; Dutoit, D. C. M.; Mallat, T.; Schneider, M.; Baiker, A. *J. Chem. Soc., Chem. Commun.* **1995**, 163.

Table 2. XPS Data of Mixed Oxides and Phosphate Incorporated Mixed Oxides

	binding energies[a]/eV					
	O 1s		Ti $2p_{3/2}$			
samples	$O_{(i)}$	$O_{(ii)}$	$Ti_{(i)}$	$Ti_{(ii)}$	Si 2p	P 2s
ST1	533.0(94)[b]	530.5(6)	461.5(25)[c]	459.1(75)	103.5	
STP1	532.6(94)	530.3(6)	461.9(24)	459.1(76)	103.5	191.2
ST2	532.6(81)	531.0(19)		459.4	103.0	
STP2	532.4(82)	530.6(18)		459.1	103.0	190.7
ST3	532.4(80)	530.6(20)		459.1	103.1	
STP3	532.4(79)	530.6(21)		459.0	103.2	190.9
TiO_2[d]		530.5		458.8		
SiO_2[e]	532.5				103.3	
Na_3PO_4[e]						190.5
Na_2HPO_4[e]						191.2
NaH_2PO_4[e]						192.3
P[e]						188.0

[a] In parentheses. [b] Relative percentage of $O_{(i)}(Si-O_{(i)})$ and $O_{(ii)}(Ti-O_{(ii)})$. [c] Relative percentage of $Ti_{(i)}$ (titanium in tetrahedral environment) and $Ti_{(ii)}$ (titanium in octahedral environment). [d] Reference 39. [e] Reference 25.

possible to observe the ν(PO) asymmetric mode, which normally occurs at ca. 1100 cm^{-1}, as it is presumably under the ν(SiO) band.

Table 2 presents the XPS data for ST and STP samples. The O 1s binding energy peaks of SiO, O(*i*), are observed between 532.4 and 533.0 eV[25] and for TiO_2, O(*ii*), are observed between 530.3 and 531.0 eV.[26−28] In ST1 (Ti = 7.7 wt %) and STP1 (Ti = 7.3 wt %), two Ti $2p_{3/2}$ binding energy peaks are observed: the first at ∼461.7 eV and the second at 459.1 eV, with relative atomic percentages of 25 and 75%. The first Ti ion is in a tetrahedral environment, and the second is in an octahedral environment.[29] For samples with more than 7.7 wt % of titanium atoms, only one Ti $2p_{3/2}$ binding energy peak at 459.1 eV is observed, indicating that all the metal is in an octahedral environment. It means that saturation of the Ti ion coordination sites may occur as the metal content in the SiO_2/TiO_2 matrixes increase due to Ti−O−Ti bond formation. In bulk phase TiO_2, where Ti ions are in an octahedral environment, only one binding energy peak at 458.8 eV is observed.[30] The P2s binding energy is observed at 191.2, 190.7, and 190.9 eV for STP1, STP2, and STP3 samples, respectively. The P 2s binding energies for various phosphate species are Na_3PO_4 = 190.5 eV, Na_2HPO_4 = 191.2 eV, NaH_2PO_4 = 192.3 eV, and elementary phosphorus P = 188.0 eV.[25] These values suggest that both PO_4^{3-} and HPO_4^{2-} species may be present in the STP samples. However, as the phosphate ions were adsorbed from an acid solution, it is less probable that PO_4^{3-} be present in the matrixes. It is well-known that titanium phosphate prepared from phosphoric acid solution is isolated as $Ti(HPO_4)_2 \cdot xH_2O$.[4,31,32]

Thermal Stability. Figure 1 shows the TGA curves for ST3 (curve A) and STP3 (curve B) is well as the corresponding DSC curves. The weight decreases of

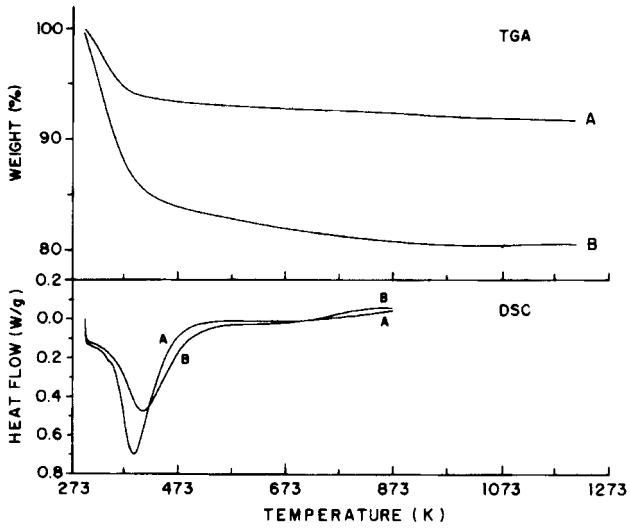

Figure 1. TGA curves: ST3 (A) and STP3 (B). Heating rate of 5 K min^{-1} under argon atmosphere. DSC curves: ST3 (A) and STP3 (B). Heating rate of 5 K min^{-1}.

∼7% (curve A) and 17% (curve B) observed at 390 K are due to loss of the hydration water. Above this temperature, up to 900 K, the small weight decreases of ∼1% (curve A) and ∼3% (curve B) correspond to structural water loss due to condensation of silanol groups.[33] Transformation of phosphate to pyrophosphate with temperature increase may also be contributing to the observed weight decrease because, as is known, titanium hydrogenphosphate submitted to heat treatment between 473 and 770 K transforms, with structural water loss, to a pyrophosphate species.[1,4,34]

The X-ray difraction patterns of the heat treated samples between 423 and 1023 K (Figure 2A−D), did not show any crystalline phase. Samples heat treated at 1273 K (Figure 2E) developed some diffraction lines. The observed peaks, in comparison with the published standard data by JCPDS,[35] are due to the crystalline phases of SiO_2 (peaks marked with a) and TiO_2 (peaks marked with b). No peaks assignable to crystalline phosphate or pyrophosphate species could be detected.

The ^{31}P NMR spectra of solid sample STP3 are shown in Figure 3a−e corresponding to the heat-treated samples at (a) 423, (b) 623, (c) 823, (d) 1023, and (e) 1273 K. Only one broadened peak centered at −8.3 ppm can be observed for the sample heat treated between 423 and 1023 K. The peak is broadened because the phosphate in the matrix is still amorphous even after heating the sample to 1023 K. The peak becomes narrower at 1273 K (Figure 3e), but, as was shown by XRD, the sample is still an amorphous species at this temperature. The peak observed at −8.3 ppm is assigned to the HPO_4^{2-} species, very similar to that recently reported for $TI(HPO_4)_2 \cdot 2H_2O$ ^{31}P NMR, where the peak was observed at −9.3 ppm.[2,36] This assignment supports the conclusion obtained from XPS data analyses. The observed

(25) *Handbook of Photoelectron Spectroscopy*; Perkin-Elmer, 1992.
(26) Shalvoy, R. B.; Reucroft, P. J.; Davis, B. H. *J. Catal.* **1978**, *56*, 336.
(27) Nefedov, V. I.; Gati, D.; Dzhurinskii, B. F.; Sergushin, N. P.; Salyn, V. V. *Russ. J. Inorg. Chem.* **1975**, *20*, 1279.
(28) Kubota, L. T.; Gushikem, Y.; de Castro, S. C.; Moreira, J. C. *Colloids Surf.* **1991**, *57*, 119.
(29) Mukhopadhyay, S. M.; Garofalini, S. H. *J. Non-Cryst. Solids* **1990**, *126*, 202.
(30) Bittar, A.; Sayari, A.; On, D.; Bonneviot, L. *Catal. Lett.* **1992**, *16*, 85.
(31) Alberti, G.; Costantino, U.; Giovagnotti, M. L. L. *Gazz. Chim. Ital.* **1980**, *110*, 61.
(32) Hosono, H.; Abe, Y. *J. Non-Cryst. Solids* **1995**, *190*, 185.
(33) Iler, R. K. *The Chemistry of Silica*; Wiley-Interscience: New York, 1979.
(34) Sanz, J.; Iglesias, J. E.; Soria, J.; Losilla, E. R.; Aranda, M. A. G.; Bruque, S. *Chem. Mater.* **1997**, *9*, 996.
(35) *Powder Diffraction File Search Manual*; published by The Joint Committee on Powder Diffraction Standards, Swarthmore, PA, 1973.

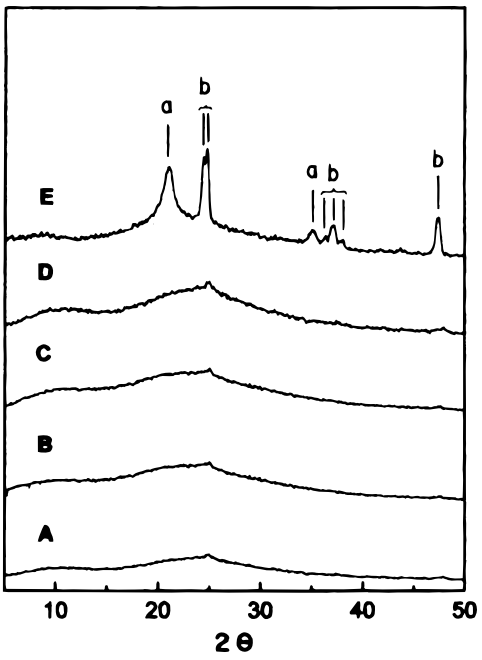

Figure 2. XRD pattern of the STP3 sample calcined at (A) 423, (B) 623, (C) 823, (D) 1023, and (E) 1273 K. Peaks marked (a) are due to the crystalline phases of SiO_2, while (b) indicates the crystalline phases of TiO_2.

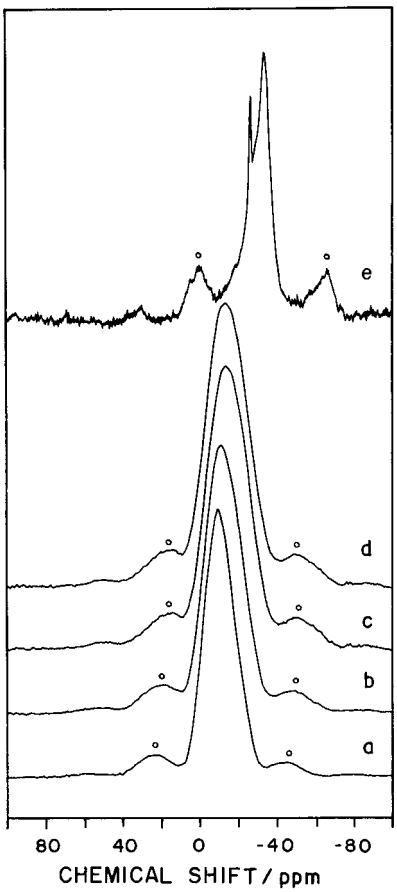

Figure 3. Cross-polarizing magic angle spinning ^{31}P NMR spectrum of solid samples of STP3 heat treated at (a) 423, (b) 623, (c) 823, (d) 1023, and (e) 1273 K. Peaks marked (○) indicates the spinning sidebands.

modification of the sample heat treated at 1273 K is not assigned to the pyrophosphate species since, for this species, the spectrum is well-known and shows a series of peaks in the region between −38 and −55 ppm.[34,37]

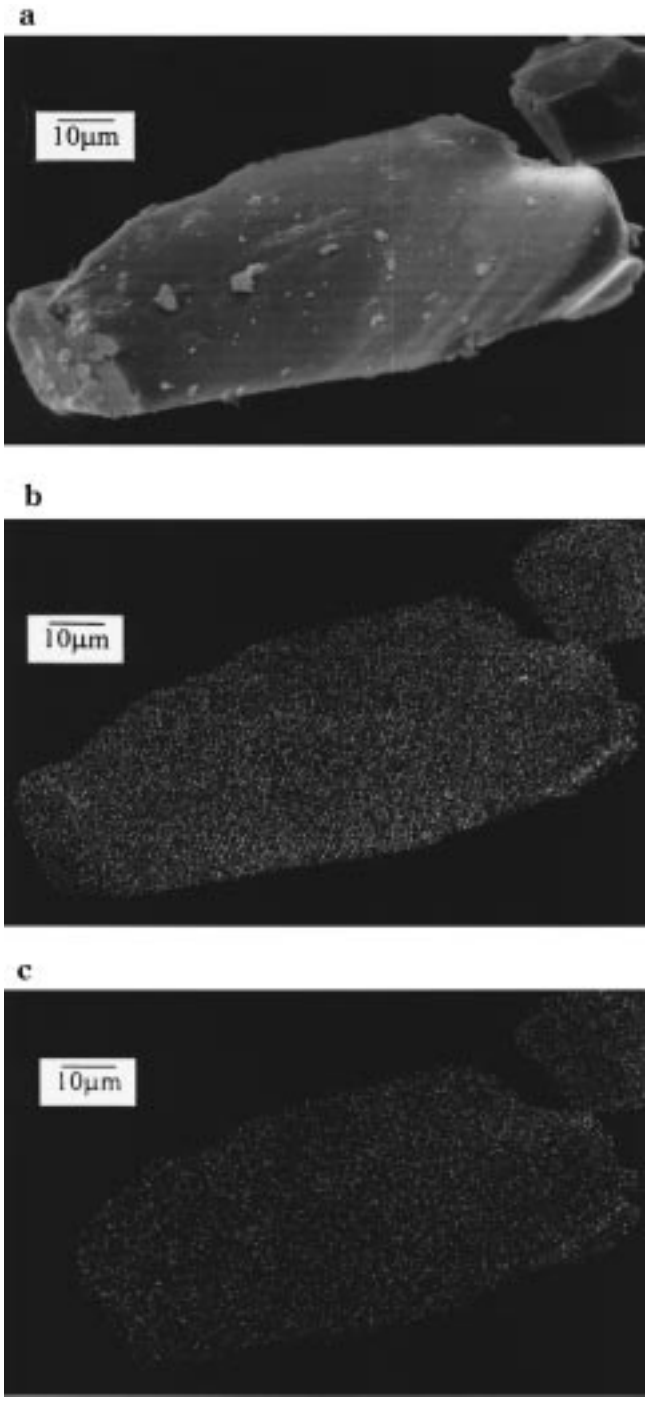

Figure 4. Scanning electron microscopy image of STP3 (a); the corresponding energy-dispersive scanning (EDS) images of titanium (b) and phosphorus (c).

Degree of Dispersion and Size of the Particles. Figure 4a show the SEM image and Figure 4b,c the corresponding EDS images of STP3. The white points in Figure 4b are due to the emission line Ti Kα = 5.52 keV and Ti Kβ = 4.93 keV, and in Figure 4c, due to the emission line PKα = 2.06 keV.[38] It is very clear that, within the magnification used, titanium atoms as well as the phosphorus atoms are highly dispersed in the

(36) Nakayama, H.; Eguchi, T,; Nakamura, N.; Yamaguchi, S.; Danjvo, M.; Tsuhako, M. *J. Mater. Chem.* **1997**, *7*, 1063.
(37) Strelko, V. V.; Khainakov, S. A.; Kvashenko, A. P.; Belyakov, V. N.; Bortun, A. I. *J. Appl. Chem. USSR* **1988**, *61*, 1922.

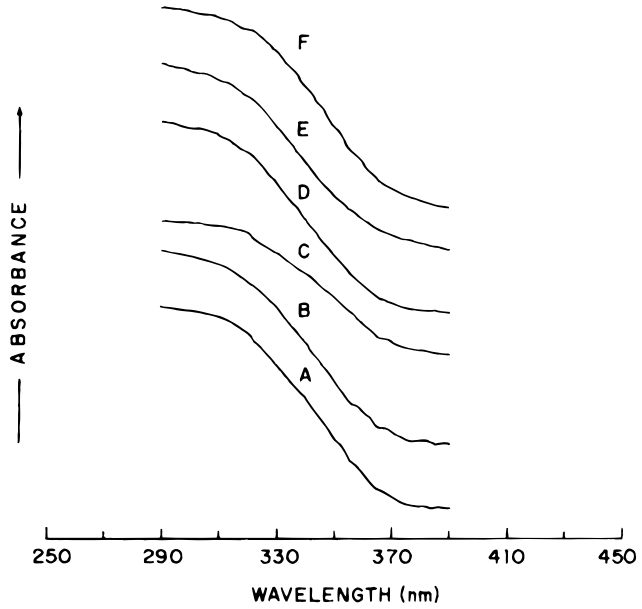

Figure 5. UV absorption spectra of ST and STP samples dispersed in spectra grade CCl_4 in 0.1 cm path length quartz cell: (A) ST1, (B) ST2, (C) ST3, (D) STP1, (E) STP2, and (F) STP3.

matrix and no evidence of islands of titanium phosphate can be detected.

Figure 5 shows the UV absorption bands for ST and STP samples with atomic ratios (calculated from XPS data) of Ti:Si between 1:7 and 1:21. Increasing the titanium atom contents in the matrix has no influence on the band threshold position at ~310 nm. In a recent work on preparation of silica−titania mixed oxides by the sol−gel process[39] for sample of SiO_2/TiO_2 with an atomic ratio of Ti:Si = 1:8 and a band threshold at ca. 330 nm, the domain size of titania particles was estimated as 1 nm. Since the UV absorption band threshold is a function of titania particle size, the same order of magnitude for the particle sizes of ST and STP is suggested in our case. The position of the band absorption threshold for bulk TiO_2 is observed at a higher wavelength, i.e., 410 nm.[40]

Conclusions

It may be concluded that HPO_4^{2-} is the species in the SiO_2/TiO_2 matrix for samples prepared and calcined between 423 and 1023 K. The reaction that leads to the formation of this species on the SiO_2/TiO_2 surface can be written as follows:

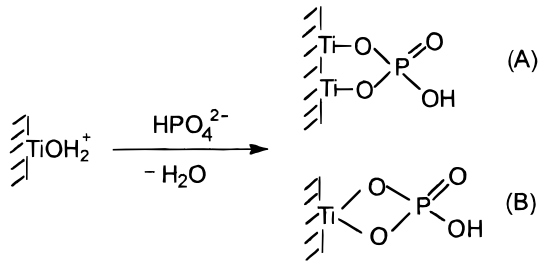

where (A) and (B) are the possible ways that hydrogenphosphate can bind to a titanium atom in the matrix. The hydrated titanium oxide is protonated at pH lower than the zero point of charge and, thus, is represented as $TiOH_2^+$.

The existence of HPO_4^{2-} species at temperatures in which it normally transforms to a pyrophosphate species is explained taking into account two aspects: the first is that (A) and/or (B) are strongly bound on the surface and thus are only slightly mobile, and second, since they are highly dispersed in the matrix, condensation to pyrophosphate does not occur below a temperature of 1273 K. In the bulk titanium hydrogenphosphate, the temperature at which condensation occurs is 470 K.[4,34] The X-ray diffraction patterns observed at 1273 K (Figure 2E) correspond to the temperature at which the phase separation of SiO_2 and TiO_2 into crystalline forms starts. The ^{31}P NMR spectrum of the sample heat treated at 1273 K (Figure 3e), which also changed at this temperature, still does not correspond to the pyrophosphate species, whose spectrum is well-known[34] and also did not appear in the XRD diffraction paterns.[4]

Acknowledgment. Y.G. is indebted to FAPESP and FINEP for financial support and A.A.S.A. to CNPq for a fellowship.

CM970679E

(38) Goodhew, P. J.; Humphreys, F. J. *J. Electron Microscopy and Analysis*, 2nd ed.; Taylor & Francis: London, 1992.

(39) da Silva, L. R. D.; Gushikem, Y.; Gonçalves, M. do Carmo; Filho, U. P. R.; de Castro, S. C. *J. Appl. Polym. Sci.* **1995**, *58*, 1669.

(40) Liu, Z.; Davis, R. J. *J. Phys. Chem.* **1994**, *98*, 1253.